Supporting Information

Swanton et al. 10.1073/pnas.0811835106

SI Methods

Data Set. Two MTS expression signatures were derived from publicly available data sets using 2 meta-analysis methods (http://www.dspace.cam.ac.uk/handle/1810/217842): MCF-7 and MDA-MB-231 breast cancer cell lines treated with docetaxel (1), ovarian cancer 1A9 xenografts treated with paclitaxel (2), the H460 non–small cell lung carcinoma cell line treated with paclitaxel (GSE 2182), and the A549 non–small cell lung carcinoma cell line treated with epothilone 906 or paclitaxel (3).

Gene Annotation and Preprocessing. The gene identifier IMAGE ID and GB_ACC number, attached by the manufacturer to each probe on the chips, was translated to Entrez Gene ID using the publicly available software MatchMiner (www.discover.nci.nih.gov/matchminer). In data sets in which multiple Entrez Gene IDs matched a single identifier, the first matching Entrez Gene ID was used based on the "chain of responsibility" in MatchMiner. This translation also was used across data sets. In cases where multiple Entrez Gene IDs matched a single identifier across data sets, the first one was selected and applied across data sets.

Meta-Analysis Methods. See http://www.dspace.cam.ac.uk/handle/1810/217842.

Binomial Test and BTPC Method. The BTPC method was used following the application of Entrez Gene IDs to each publicly available data set. The BTPC method delivers a number of genes that are differentially expressed across experiments in one direction and that exhibit a significant difference in expression level compared with control samples. In the first step, the ordinary binomial test was calculated for each gene using the dichotomized fold change values (-1 for negative fold change and 1 for positive fold change) and a significance threshold of $P \leq .05$. Each gene was assessed for differential expression using the moderated t-test, implemented in the limma package in Bioconductor. The moderated t test uses a nonparametric empirical Bayes method to shrink the estimated sample variances toward a pooled estimate, resulting in more stable inference when the number of replicates is small. Based on the moderated t-test, the P values for each gene were calculated and adjusted for multiple testing by calculating a q-value (4). To account for the quality of the data sets, the q-values were weighted based on a measure of the spread (the interquartile range). To filter the genes in a second step, a threshold of the weighted mean q-values was used, delivering the signature.

Next, a permutation-based false discovery rate (FDR) was calculated to control the genes identified by chance alone. To perform the experiment label permutation simulation, the gene identifiers within one data set were separated from the values and randomly reassigned. In each permutation, a number of genes appeared, tagged to be significantly differentially expressed even though they were identified by chance alone. Ten permutations were performed, and the FDR was calculated for each permutation. The arithmetic mean across all FDRs delivers the overall FDR and thus the percentage of false-positive results within the significant genes. Three other meta-analysis methods were examined and validated by the FDR, but the BTPC method delivered the lowest FDR for both up-regulated and down-regulated genes. The SDs and 95% confidence intervals for the FDRs also were calculated for each meta-analysis method. The R-script for the BTPC method is enclosed within the file available at http://www.dspace.cam.ac.uk/handle/1810/217842.

Rank Method. The rank method delivers a number of genes that are regulated with a specific difference from control samples. The genes in each experiment were sorted by the fold change values, and a rank was calculated for each gene. Genes were selected based on a rank threshold of 20. Genes were selected for the signature if they appeared in half or more of the data sets and if in all of those data sets, the genes were consistently regulated in one direction with no assessment of significance level.

CIN Signature. The published CIN signatures (CIN70 and CIN27wp) and an extended gene list incorporating the top 5%, 10%, and 15% of genes overexpressed in the CIN signature were used in this analysis (5). Genes were excluded from the final signature (wp) if they were identified as cell cycle–regulated transcripts, resulting in a final gene list of CIN382wp, CIN826wp, and CIN1264wp (6).

TaqMan Low-Density Arrays. HCT116 *hSecurin*$^{+/+}$ and *hSecurin*$^{-/-}$, A549, HCC-2998, SW620, COLO205, HCT-15, KM12, MCF7, MDA-MB-231, HS578T, and BT549 cells were plated at 3×10^6 cells per 10-cm plate. After 24 h, the cells were treated for an additional 24 h with 0.5× of the cell-specific GI50 of paclitaxel. Total RNA was extracted and cDNA was synthesized as described above. The TaqMan Low-Density Arrays (TLDAs; Applied Biosystems) used allowed simultaneous quantification of 8 samples against 47 preloaded specifically designed TaqMan assays, with an additional 18S RNA and GAPDH TaqMan assay to detect the endogenous controls. For each port, 100 μL of reaction mixture (containing 2 μL of the 20-μL room temperature reaction and 2× TaqMan Universal PCR MasterMix) was added. The cards were run on the TLDA block of an Applied Biosystems 7900 HT real-time PCR system.

Cell Culture and siRNA Transfection. HCT-116 wild-type and isogenic *hSecurin*$^{-/-}$ isogenic cells (7) were cultured in DMEM supplemented with 10% FBS, 2 mM L-glutamine, 100 μg/mL of streptomycin, and 100 U/mL of penicillin at 37 °C and 10% CO_2. All other cell lines used in this study were from the NCI60 cell panel and were cultured in RPMI medium supplemented with 10% FBS, 2% bicarbonate, 2 mM L-glutamine, 100 μg/mL of streptomycin, and 100 U/mL of penicillin at 37 °C and 5% CO_2.

The siRNA (25 nM)–DharmaFect1 (both from Dharmacon) transfection mixture was pipetted, after which 4.5×10^3 of HCT-116 cells per well of a 96-well plate or 3×10^5 of HCT116 cells per well of a 6-well plate in antibiotic-free media was added. Cells were either processed for analysis or drug-treated 48 h after transfection.

Quantification of siRNA Cytotoxicity and Acumen Explorer Analysis. HCT-116 cells were plated at 6,000 cells/well in 96-well plates pretreated with poly-L-lysine, then subjected to reverse transfection with 25 nM siRNA–DharmaFect1 transfection reagent (Dharmacon) according to the manufacturer's instructions. Scrambled nontargeting and RNA- induced silencing complex–free controls were used for each experiment. At 48 h posttransfection, cells were prepared for analysis in the Acumen Explorer laser cytometer. After medium was aspirated from the cells, 100 μL of 80% ethanol in PBS at -20 °C was added to each well, and the cells were incubated at -20 °C for 30 min. Each well was then washed twice in PBS, after which 100 μL of 0.2 mg/ml RNase in PBS was added to each well and incubated for 1 h at 37 °C. The RNase solution was then aspirated, and 100 μL of 10 μM

propidium iodide was added to each well. The plate was incubated in the dark for 15 min before being analyzed for quantification of cell number and cell cycle profile. The plates were scanned using a 488-nm laser at a sampling resolution of 1 μm in the X direction and 8 μm in the Y direction. The whole well was selected for scanning. Cells were identified on the basis of size measurements, to exclude debris and large clusters of cells from analysis. This cell population was then subdivided into subG1, G1, S, G2/M, >4n, and 8n subpopulations based on the total intensity readout from each cell. The data were exported to give the percentage of cells in each phase of the cell cycle within a well.

Determination of subG1 Cells and Polyploidy by Flow Cytometry. Cells were fixed with 70% ethanol and incubated with 6 μg/mL of anti–MPM-2 antibody (Upstate) diluted in PBS/0.2%BSA for 1 h. The cells were then washed and incubated with Alexa Fluor 488–conjugated antibody (Invitrogen) diluted in PBS containing 50 μg/mL of RNaseA and 50 μg/mL of propidium iodide, and then analyzed with a BD LSRII flow cytometer. Cell doublets and debris were excluded from analysis on the basis of their pulse height and area, and at least 3×10^4 events were recorded.

RNA Extraction and cDNA Synthesis. Total RNA was extracted using the Qiagen RNeasy system following the manufacturer's instructions. An Applied Biosystems high-capacity cDNA RT kit was used to synthesize cDNA from 1 μg of total RNA.

Survival Analysis. The mean of the logged expression levels of CIN-survival or MTS-repressed genes was taken as a single prognostic factor and tested as a predictor of long-term outcome in 8 previously published data sets (8–15). Similar to Carter et al. (5), patients were divided into 2 groups, those above and those below the median of the average CIN-survival or MTS expression signature gene expression. For each cohort, the prognostic effects of these MTS-repressed genes were examined using Kaplan-Meier survival analysis (16) and the Cox proportional hazard model (17). The Sweave analysis is enclosed within the file available at http://www.dspace.cam.ac.uk/handle/1810/217842.

Classification of Genomic Instability Status by DNA Image Cytometry. Each tumor was classified as belonging to 1 of 3 groups: (*i*) diploid, with a distinct peak in the normal 2c region and no cells exceeding 5c; (*ii*) aneuploid, with a main peak different from 2c and a stemline scatter index (SSI) ≤8.8; or (*iii*) aneuploid, with varying numbers of cells (>5%) exceeding 5c (SSI 8.8). This novel classification system adheres to the parameters established by Kronenwett et al. (18), who defined the SSI as a measurement of clonal heterogeneity in a tumor cell population.

1. Hernandez-Vargas H, Palacios J, Moreno-Bueno G (2007) Molecular profiling of docetaxel cytotoxicity in breast cancer cells: Uncoupling of aberrant mitosis and apoptosis. *Oncogene* 26:2902–2913.
2. Bani MR, et al. (2004) Gene expression correlating with response to paclitaxel in ovarian carcinoma xenografts. *Mol Cancer Ther* 3:111–121.
3. Chen JG, Yang CP, Cammer M, Horwitz SB (2003) Gene expression and mitotic exit induced by microtubule-stabilizing drugs. *Cancer Res* 63:7891–7899.
4. Storey JD, Tibshirani R (2003) Statistical significance for genomewide studies. *Proc Natl Acad Sci USA* 100:9440–9445.
5. Carter SL, Eklund AC, Kohane IS, Harris LN, Szallasi Z (2006) A signature of chromosomal instability inferred from gene expression profiles predicts clinical outcome in multiple human cancers. *Nat Genet* 38:1043–1048.
6. Whitfield ML, et al. (2002) Identification of genes periodically expressed in the human cell cycle and their expression in tumors. *Mol Biol Cell* 13:1977–2000.
7. Jallepalli PV, et al. (2001) Securin is required for chromosomal stability in human cells. *Cell* 105:445–457.
8. Ivshina AV, et al. (2006) Genetic reclassification of histologic grade delineates new clinical subtypes of breast cancer. *Cancer Res* 66:10292–10301.
9. van de Vijver MJ, et al. (2002) A gene-expression signature as a predictor of survival in breast cancer. *N Engl J Med* 347:1999–2009.
10. Miller LD, et al. (2005) An expression signature for p53 status in human breast cancer predicts mutation status, transcriptional effects, and patient survival. *Proc Natl Acad Sci USA* 102:13550–13555.
11. van't Veer LJ, et al. (2002) Gene expression profiling predicts clinical outcome of breast cancer. *Nature* 415:530–536.
12. Naderi A, et al. (2007) A gene-expression signature to predict survival in breast cancer across independent data sets. *Oncogene* 26:1507–1516.
13. Chin K, et al. (2006) Genomic and transcriptional aberrations linked to breast cancer pathophysiologies. *Cancer Cell* 10:529–541.
14. Wang Y, et al. (2005) Gene-expression profiles to predict distant metastasis of lymph-node-negative primary breast cancer. *Lancet* 365:671–679.
15. Bild AH, et al. (2006) Oncogenic pathway signatures in human cancers as a guide to targeted therapies. *Nature* 439:353–357.
16. Kaplan EL, Meier P (1958) Nonparametric estimation from incomplete observations. *J Am Stat Assoc* 53:437–481.
17. Cox DR, Oakes D (1984) *Analysis of Survival Data* (Chapman & Hall, New York).
18. Kronenwett U, et al. (2004) Improved grading of breast adenocarcinomas based on genomic instability. *Cancer Res* 64:904–909.

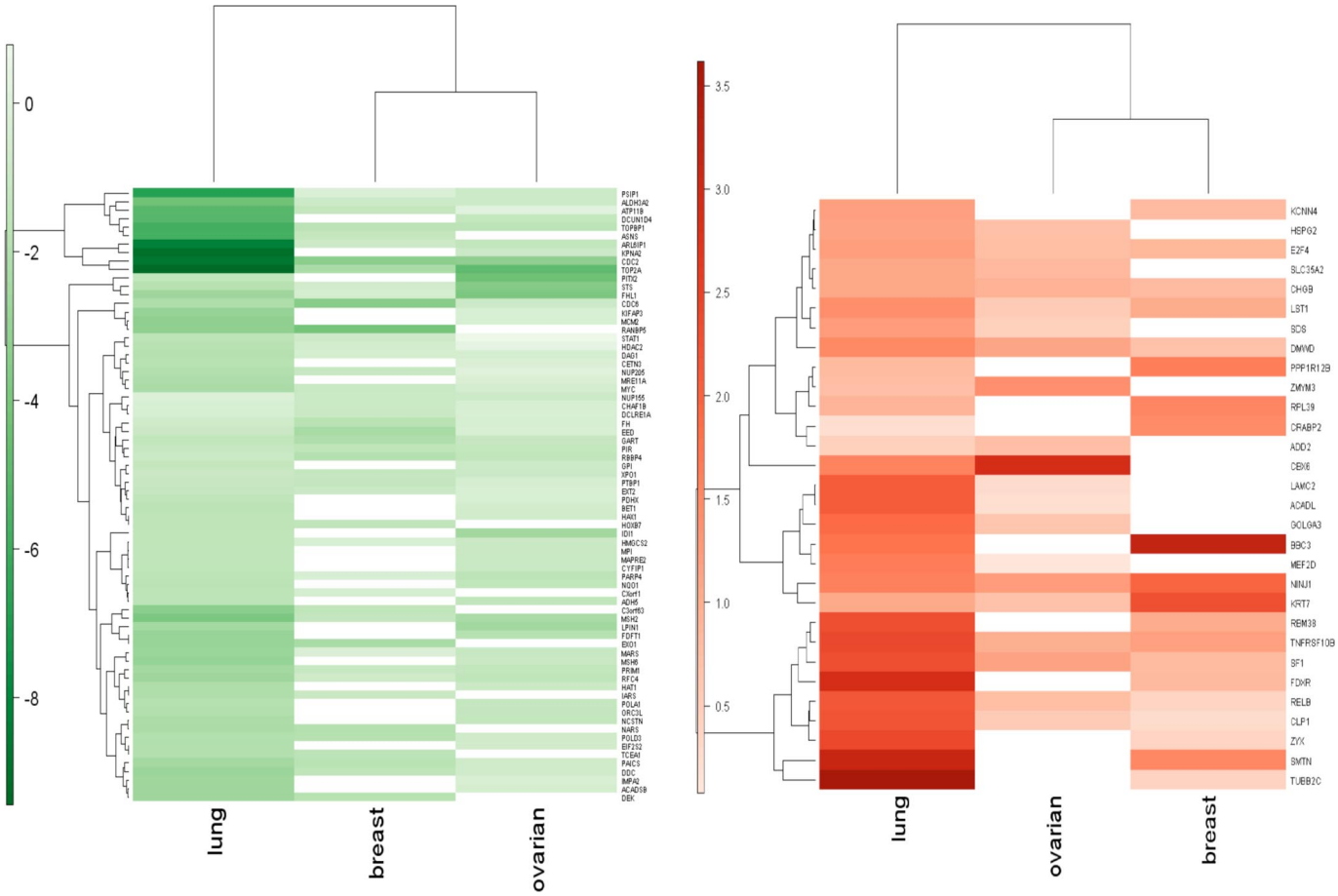

Fig. S1. BTPC MTS expression signature demonstrating the most significant repressed and expressed genes following MTS exposure in the 5 data sets. Shown are heat maps reflecting gene expression changes with log2 fold change values of significantly up-regulated (red) or down-regulated (green) genes in the rows and tumor cell line data sets in the columns, both sorted by hierarchical clustering with Euclidean distance (www.bioconductor.org). White cells indicate that this gene was not included on the microarray or removed in the filtering step before the meta-analysis.

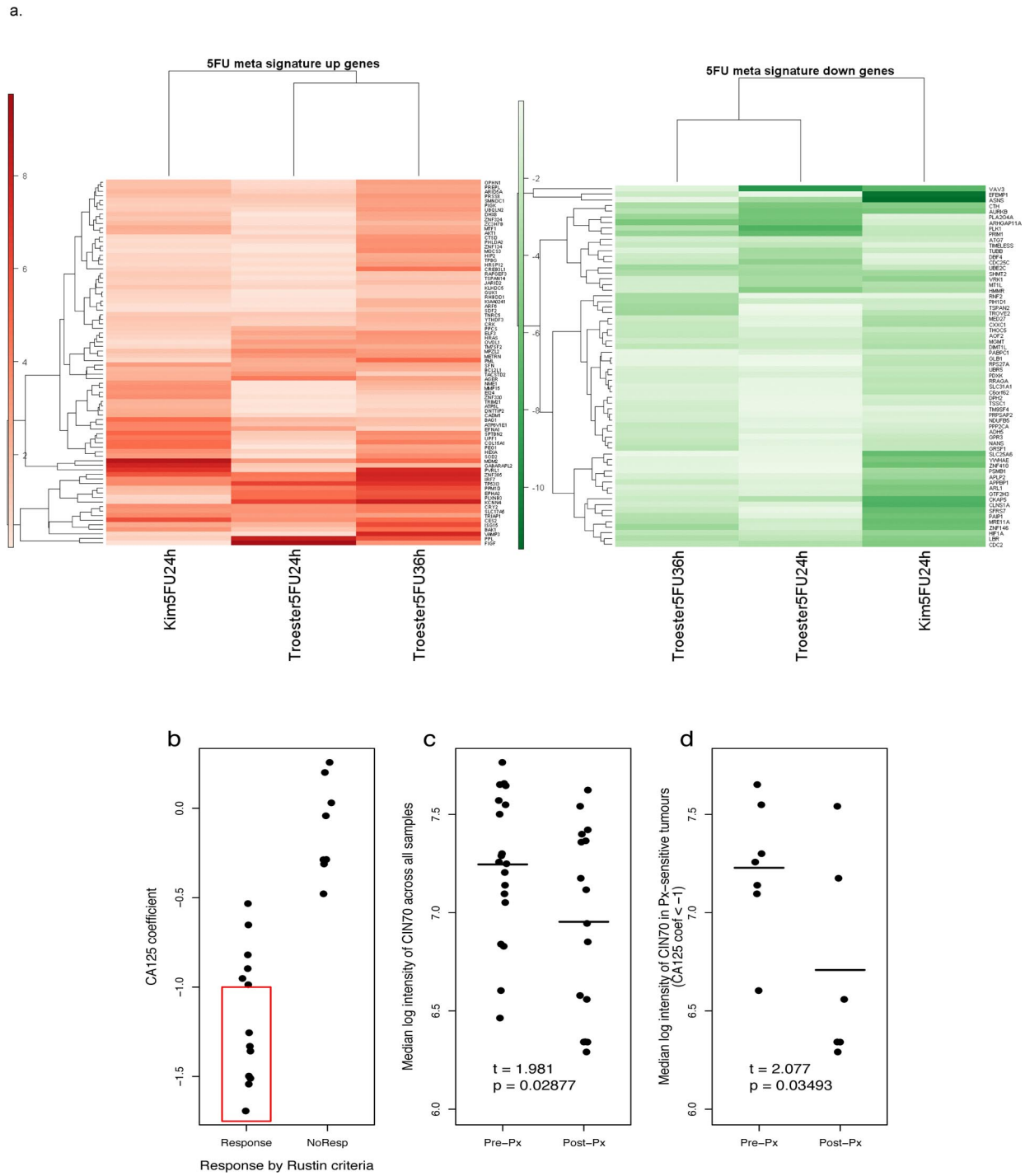

Fig. S2. (*A*) BTPC expression signature demonstrating the most significant repressed and expressed genes following 5-FU exposure in the 3 data sets. Shown are heat maps reflecting gene expression changes with log2 fold change values of significantly up-regulated (red) or down-regulated (green) genes in the rows and tumor cell line data sets in the columns, both sorted by hierarchical clustering with Euclidean distance (www.bioconductor.org). (*B*) To quantify tumor response, an exponential model was fitted for each patient to the CA125 tumor marker over three cycles of treatment. The resulting coefficient is concordant with the response criteria defined by Rustin et al. (1) and was used to identify the most paclitaxel-sensitive patients (red box). (*C*) The median expression of the CIN70 genes is decreased in posttreatment tumors relative to pretreatment tumors, (*D*) especially in those patients with the most paclitaxel-sensitive disease (boxed in red in *B*). Statistics shown are one-sided t-tests. Horizontal bars indicate mean values.

1. Rustin GJ, et al. (2004) Re: New guidelines to evaluate the response to treatment in solid tumors (ovarian cancer). *J Natl Cancer Inst* 96:487–488.

a.

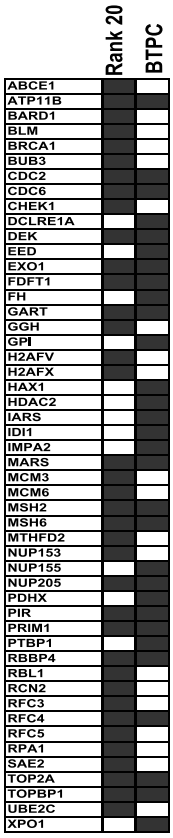

b.

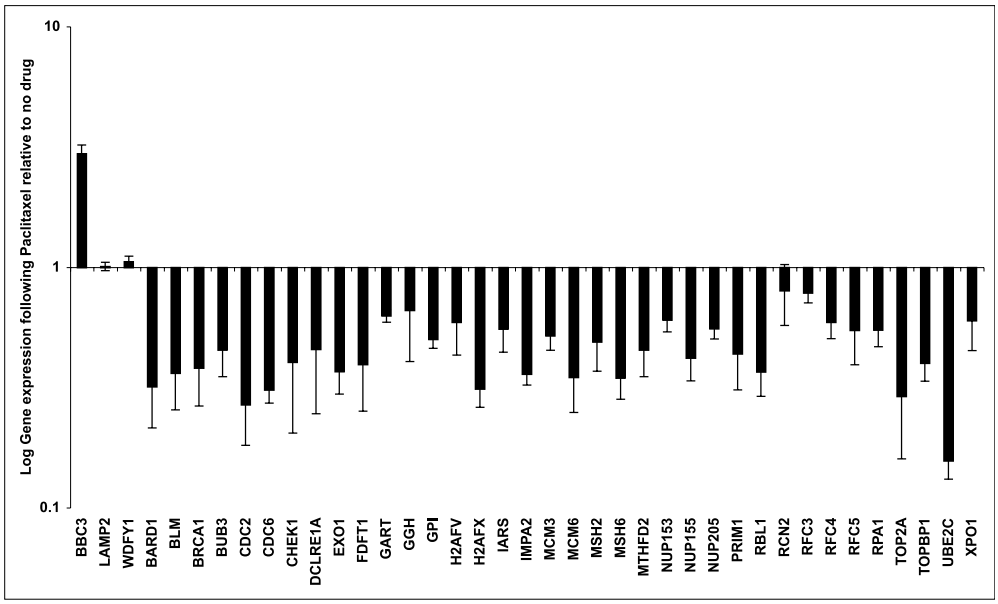

Fig. S3. (*A*) Summary of genes repressed by MTS using 2 meta-analysis methods that are overexpressed in the top 15% of genes expressed in CIN tumors with proliferation genes removed. The list of 50 genes repressed in the MTS expression signatures derived from the 2 methods that are overexpressed in CIN tumors as part of the CIN signature were chosen for further functional analysis using RNA interference (5). (B) Validation of MTS expression signature–repressed genes in the HCT-116 colorectal cancer cell line. Shown is the log fold change in gene expression (± 1 SD) determined by TLDA qPCR analysis of genes normalized to 18s RNA expression derived from the 2 MTS expression signatures following 24 h of paclitaxel treatment (50 nM) in 3 biological replicate experiments compared with gene expression in vehicle (DMSO) control treated HCT-116 cells. BBC3/Puma, a known taxane-induced gene derived from our metasignature, and *LAMP2* and *WDFY1* (genes whose expression is not influenced by taxane exposure; C.S. and J.D., unpublished data) were used as controls.

a.

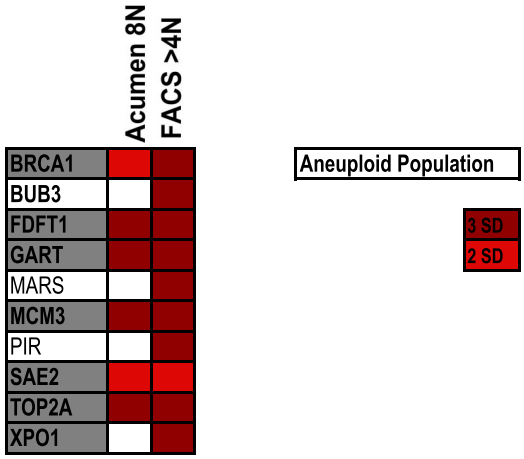

b.

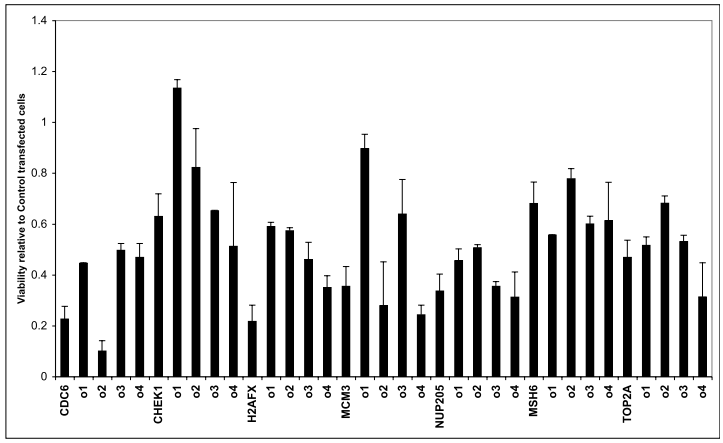

c.

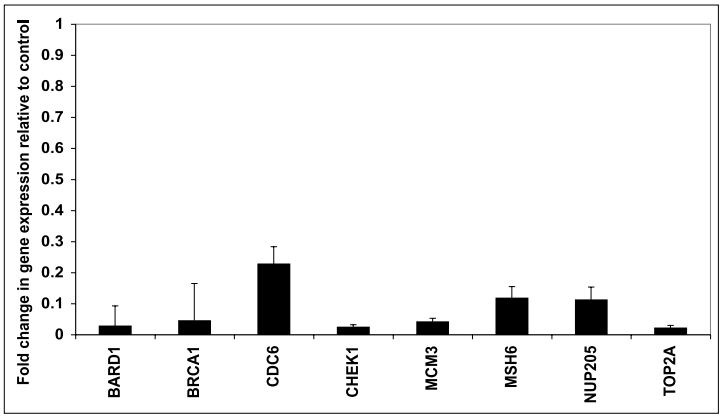

Fig. S4. (*A*) MTS-repressed genes promote aneuploidy and cell death when silenced by siRNA. Genes repressed within the 2 MTS expression signatures that are overexpressed in CIN tumors significantly increased the fraction of aneuploid cells assessed by Acumen and flow cytometry when silenced using RNAi. CIN-survival genes are highlighted in gray. The lower limit of SD of the mean percentage of aneuploid cells from 3 independent experiments is greater than the mean aneuploid population in control transfected cells + 2 SDs (light red) or + 3 SDs (dark red) from 3 independent experiments. (*B*) Deconvolution of siRNA smartpools and assessment of cell viability. The experiments shown in Fig 2(*B*) were repeated with the deconvoluted siRNA sequences from the Smartpool. An Acumen Explorer laser cytometer was used to quantify viable cells 72 h after transfection of the Smartpool siRNA targeting the gene of interest. SDs are displayed for 2 independent experiments. (*C*) Assessment of target silencing. Fast SYBR green real-time PCR quantification of target silencing (+ 1 SD from 3 independent transfections) was confirmed 72 h after transfection of HCT-116 cells with siRNAs, conferring an effect on cell viability, cell death, or aneuploidy compared with gene expression in nontargeting control siRNA-transfected cells.

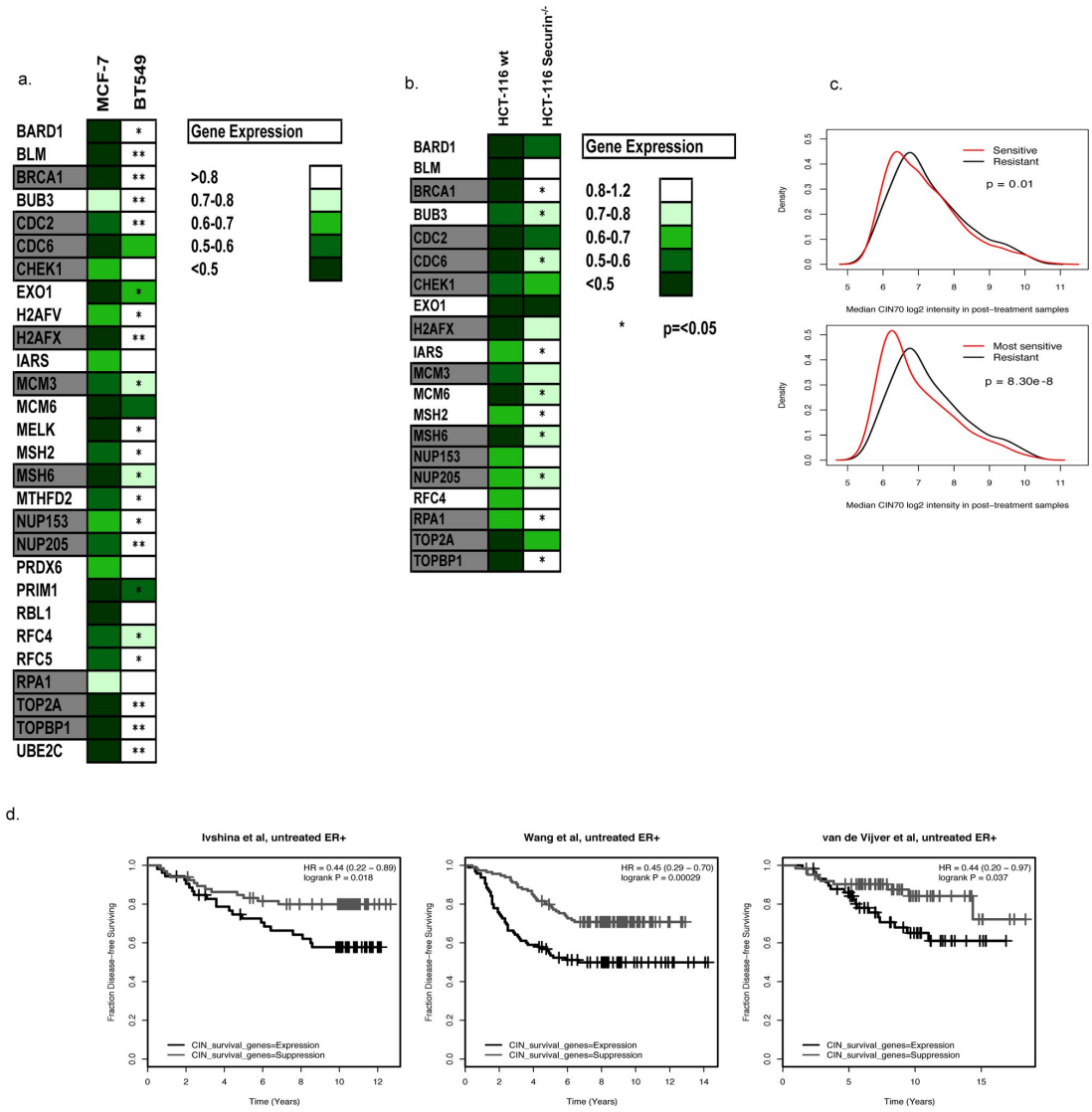

Fig. S5. (*A*) Quantification of gene repression following paclitaxel treatment of MCF-7 and BT549 cell lines. Fold change in gene expression post–paclitaxel treatment (24 h) relative to expression in vehicle control treated cells was determined by TaqMan qPCR analysis (normalization to GAPDH) following 24 h of paclitaxel treatment (concentration, 50% of the Gi50 dose) in 3 biological replicate experiments in the MCF-7 (CIN^{low}) and BT549 (CIN^{high}) breast cancer cell lines. Color-coding represents the mean fold change in gene expression of 3 biological replicates relative to cells treated with vehicle alone (+1 SD). CIN-survival genes are highlighted in gray. The significance of differential gene repression compared with the MCF-7 cell line after paclitaxel treatment is determined by the 2-tailed Student *t*-test: $*P < 0.05$; $**P < 0.005$. (*B*) Impaired repression of MTS-cytotoxic CIN-survival genes after paclitaxel treatment in an isogenic model of CIN. Quantification of gene repression following treatment of HCT-116 wild-type parental cells compared with HCT-116 isogenic *hSecurin* (−/−) after 24 h of paclitaxel treatment (50 nM) normalized to 18s. Color-coding represents the mean fold repression + 1 SD from 3 biological replicates. *P* values ($*P < 0.05$) indicate significantly greater gene repression in the HCT-116 parental cell line (1-tailed Student *t*-test). (*C*) Residual CIN expression posttreatment is higher in paclitaxel-resistant compared to paclitaxel-sensitive tumors. (*Upper*) Sensitivity defined by the Rustin criteria: The distribution of log2 intensities of CIN70 genes in residual tumors following paclitaxel across all Rustin-resistant (black line) and Rustin-sensitive (red line) patients. (Kolmogorov-Smirnov test, $D = 0.11$, $P = 0.01$). (*Lower*) Sensitivity defined by the CA125 coefficient: The same analysis was applied to taxane-resistant (black line: CA125 coefficient >-0.5) and patients most sensitive to paclitaxel (red line: CA125 coefficient <-1, see Fig. S2*B*) (Kolmogorov-Smirnov test, $D = 0.22$, $P = 8.30e\text{-}8$). (*D*) Expression of CIN-survival genes correlates with poorer survival in breast cancer. The mean of the logged expression levels of CIN-survival genes was taken as a single prognostic factor and tested as a predictor of outcome in 4 untreated Estrogen receptor positive breast cancer cohorts. Similar to the study of Carter et al. (5), patients were divided into 2 groups with above- or below-median expression of the CIN-survival gene signature expression, and the prognostic effects were examined using Kaplan-Meier survival analysis and the Cox proportional hazard model (17). Shown are 3 significant Kaplan-Meier graphs from the 4 cohorts analyzed.

Table S1a. Data sets used to derive the MTS response signature

Primary cancer	Cell line	Author	Array type	Number of genes on platform	Time points	Drug type	Concentration	Sample number
Breast	MCF7	Hernández-Vargas et al. (1)	CDNA Oncochip	7463	24 h, 48 h	Docetaxel	4 nM	4
	MCF7				24 h, 48 h	Docetaxel	100 nM	4
	MDA-MB-231				24 h, 48 h	Docetaxel	100 nM	4
Ovary	1A9	Bani et al. (2)	CDNA NCI	4535	24 h	Paclitaxel	60 mg/kg	17
NSCLC	H460	Kim et al.	CDNA Digital Genomics	7008	24 h	Paclitaxel	5 nM	2
NSCLC	A549	Chen et al. (3)	Affymetrix U95Av2		18 h	Paclitaxel	4 nM, 8 nM	3
	A549			9089	18 h	Paclitaxel	16 nM, 45 nM	2
	A549				18 h	Epothilone	40 nM	2

Shown are the cell lines treated with the MTS (and study authors), the type of array used to derive each gene expression signature (cDNA or Affymetrix), the number of genes on the platform, the duration and concentration of drug exposure, and the number of biological replicates for each experiment.

Table S1b. Genes overexpressed in CIN tumors are significantly repressed following MTS treatment across all data sets

CIN list	Test statistic *D*/quantity of difference	*P* value
CIN27WP	0.2408	3.28e-07
CIN382WP	0.1299	< 2.2e-16
CIN826WP	0.0942	< 2.2e-16
CIN1264WP	0.0753	< 2.2e-16

Cell cycle–regulated genes were removed from the CIN70 signature resulting in the signature of the top 5% (CIN382wp), 10% (CIN826wp), and 15% (CIN1264wp) of overexpressed genes in CIN tumors. The empirical frequency distribution of CIN27wp, CIN382WP, CIN826wp, and CIN1264wp signature genes was compared with the gene expression changes across all data sets following MTS exposure using the 1-sided bootstrap Kolmogorov-Smirnov test. The test statistics and *P* values for the Kolmogorov-Smirnov test reveal a significant left shift of the empirical frequency distribution of the CIN genes, indicating a greater likelihood of CIN-signature gene repression following MTS treatment.

Table S1c. Genes overexpressed in CIN tumors are significantly repressed in MTS expression signatures but not in a 5-FU signature

Meta-analysis	Number of repressed genes after filtering	*P* value	
		CIN27wp	CIN382wp
MTS rank 20	152	.0027 (4)	.0018 (18)
MTS BTPC	72	9.2e-05 (4)	1.0e-08 (16)
5-FU BTPC	64	.18 (1)	.06 (5)

Genes whose expression is influenced by cell cycle phase (6) were removed from the CIN70 signature and the signature of the top 5% (CIN382wp) of overexpressed genes in CIN tumors. Repression of genes in the CIN signature derived from 2 MTS meta-analysis signature methods (rank and BTPC), with the number of repressed genes after filtering demonstrated for each meta-analysis method shown. Three gene expression data sets were used to derive a 5-FU signature using the BTPC method. The table demonstrates the level of significance for the representation of MTS or 5-FU-repressed genes in the CIN signature. *P* values indicate the significance of the association of the CIN signature genes within the MTS or 5-FU expression signatures of repressed genes using the 1-sided Fisher's exact test, with the number of genes overlapping with each CIN data set given in parentheses.

Table S1d. Repression of CIN genes occurs preferentially in taxane-sensitive xenografts.

	Resistant xenograft		Sensitive xenograft	
CIN list	Test statistic	*P* value	Test statistic	*P* value
CIN27WP	0.31	.26	0.20	.56
CIN382WP	0.08	.32	0.16	.01*
CIN826WP	0.09	.047*	0.14	.001**
CIN1264WP	0.05	.19	0.11	.0006***

Publicly available expression data deriving from paclitaxel-treated human ovarian cancer xenografts in nude mice (2) were analyzed for repression of genes overexpressed in CIN tumors following paclitaxel treatment. The sensitive ovarian cancer cell line (1A9) and its paclitaxel-resistant derivative (1A9PTX22) were treated with 60 mg/kg of paclitaxel, which resulted in tumor responses in 1A9 tumors but not in 1A9PTX22 xenografts. *P* values are given for the Kolmogorov-Smirnov test comparing the distribution of genes overexpressed in the CIN signature (with proliferation genes excluded) with the distribution of genes having a negative fold change in ovarian cancer xenografts following paclitaxel treatment of nude mice. CIN genes are significantly repressed in taxane-sensitive ovarian cancer xenografts but less significantly in the paclitaxel-resistant xenograft model.

Table S2. The Gi50 for each cell line and the concentrations of paclitaxel used in each cell line (nM) relative to the cell line Gi50

Cell line	0.25×	0.5×	Gi50
HCT116	12.5	25	50
HCT15	50	100	200
KM12	50	100	200
HCC2998	50	100	200
SW620	100	200	400
COLO205	100	200	400

Table S3. Summary of clinical and experimental parameters in 14 dGS, 14 aGS, and 16 aGU breast carcinomas (see SWEAVE analysis)

Ploidy	Age	Size, mm	Elston grade	Histology	Side	Lymph node metastasis	ER	PR	Centroid
dGS	61	ND	II	Ductal	Left	0/0	Pos	Pos	Norm
dGS	83	30	II	Ductal	Right	0/3	Pos	Pos	LumA
dGS	41	18	II	Mucin	Left	0/11	Pos	Pos	LumA
dGS	51	12	ND	Lobular	Right	0/8	Neg	Neg	Norm
dGS	48	25 x 20	II	Lobular	Left	0/0	Pos	Pos	LumA
dGS	75	12	I	Tubular	Right	0/0	Pos	Pos	LumA
dGS	86	10	ND	Lobular	Left	0/0	Pos	Neg	LumB
dGS	86	26	I	Ductal	Right	4/6	Pos	Pos	LumA
dGS	50	ND	II	Lobular	Right	3/9	Pos	Pos	Norm
dGS	54	70	III	Lobular	Left	1/12	Pos	Pos	LumA
dGS	62	20	I	Ductal	Right	0/3	ND	ND	LumA
dGS	79	22	II	Ductal	Left	4/16	Pos	ND	LumA
dGS	34	10	II	Ductal	Left	0/0	Pos	Pos	LumA
dGS	71	12	I	Lobular	ND	0/0	Pos	Pos	ERBB2
aGS	55	60	III	Ductal	Right	9/9	Pos	Neg	LumA
aGS	62	11	I	Ductal	Right	0/23	Pos	Pos	LumA
aGS	72	15	II	Ductal	Left	0/5	Pos	Pos	LumA
aGS	58	14	I	Ductal	Left	0/0	Pos	Pos	LumA
aGS	71	ND	II	Paget's	Right	0/0	Pos	Pos	ERBB2
aGS	81	26	II	Ductal	Left	1/7	Pos	Pos	LumA
aGS	62	60 + 15	I	Lobular	Right	2/7	Pos	Pos	LumA
aGS	75	13	I	Ductal	Left	0/0	Pos	Pos	LumA
aGS	54	12 + 9	II	Ductal	Right	0/0	Pos	Neg	LumA
aGS	49	54	III	Ductal/lobular	Right	0/0	Neg	Pos	Norm
aGS	52	14	II	Ductal	Right	0/6	Pos	Pos	LumA
aGS	63	30	II	Ductal	Left	0/0	ND	ND	Norm
aGS	43	20	III	Ductal	Left	0/6	Pos	Neg	LumA
aGS	88	20	III	Ductal	Left	0/0	Pos	Pos	LumA
aGU	54	20	III	Ductal	Right	0/5	Neg	Neg	Basal
aGU	62	35	III	Comedo	Right	0/35	Pos	Pos	ERBB2
aGU	43	35	III	Ductal	Left	0/0	Neg	Pos	Basal
aGU	46	20	III	Ductal	Left	0/0	Neg	Neg	Basal
aGU	54	30	III	Medullary	ND	14/15	Neg	Neg	Basal
aGU	74	40	III	Ductal	Left	0/17	Neg	Neg	Basal
aGU	55	40	III	Ductal	Right	0/0	Pos	Pos	LumB
aGU	71	30	III	Ductal	Left	0/0	Pos	Pos	LumB
aGU	79	16	III	Ductal	Left	4/14	Pos	Pos	ERBB2
aGU	57	25	III	Ductal	Left	0/2	Neg	Neg	ERBB2
aGU	59	20	III	Ductal	Left	1/9	Neg	Neg	ERBB2
aGU	85	45	III	Comedo	Right	0/3	Neg	Neg	Basal
aGU	66	12	III	Lobular	Left	0/0	Pos	Pos	Norm
aGU	62	12	II	Ductal	Right	0/10	Neg	Neg	Basal
aGU	60	18 + 9	III	Ductal	ND	0/ND	Neg	Neg	Basal
aGU	57	8	III	Metaplastic	Right	0/0	Neg	Neg	Basal

ER, estrogen receptor; PR, progesterone receptor; Pos, positive; Neg, negative; ND, not determined.